

**FINAL**

CONF-820274--1

CONF-820274--1

DEFECTS IN METALS\*

DE83 007638

R. W. Siegel  
Materials Science Division  
Argonne National Laboratory  
Argonne, Illinois 60439, USA

The submitted manuscript has been authored  
by a contractor of the U.S. Government  
under contract No. W-31-109 ENG-38.  
Accordingly, the U. S. Government retains a  
nonexclusive, royalty-free license to publish  
or reproduce the published form of this  
contribution, or allow others to do so, for  
U. S. Government purposes.

JUNE 1982

### **DISCLAIMER**

This report was prepared as an account of work sponsored by an agency of the United States Government. Neither the United States Government nor any agency thereof, nor any of their employees, makes any warranty, express or implied, or assumes any legal liability or responsibility for the accuracy, completeness, or usefulness of any information, apparatus, product, or process disclosed, or represents that its use would not infringe privately owned rights. Reference herein to any specific commercial product, process, or service by trade name, trademark, manufacturer, or otherwise does not necessarily constitute or imply its endorsement, recommendation, or favoring by the United States Government or any agency thereof. The views and opinions of authors expressed herein do not necessarily state or reflect those of the United States Government or any agency thereof.

### **NOTICE**

**PARTS OF THIS REPORT ARE ILLEGIBLE. IT  
has been reproduced from the best available  
copy to permit the broadest possible avail-  
ability.**

\*This work was supported by the U.S. Department of Energy.

To be published in Positron Annihilation Spectroscopy, the Proceedings of the Second National Symposium on Positron Annihilation, Madras, India, 8-12 February 1982. INVITED PAPER.

**MASTER**

SP

## DEFECTS IN METALS\*

R. W. Siegel  
Materials Science Division  
Argonne National Laboratory  
Argonne, Illinois 60439, USA

### ABSTRACT

The application of positron annihilation spectroscopy (PAS) to the study of defects in metals has made significant contributions to our knowledge regarding lattice-defect properties during the past decade. These contributions have been primarily in two areas: (i) the determination of atomic defect properties, particularly those of monovacancies, and (ii) the monitoring and characterization of vacancy-like microstructure development during post-irradiation and post-quench annealing. The study of defects in metals by PAS is selectively reviewed within the context of the other available techniques for defect studies. The strengths and weaknesses of PAS as a method for the characterization of defect microstructures are considered vis-a-vis some of the other tools of the materials scientist. The additional possibilities for using the positron as a localized probe of the atomic and electronic structures of atomic defects are discussed, based upon theoretical calculations of the annihilation characteristics of defect-trapped positrons and experimental observations. Finally, the present status and future potential of PAS as a tool for the study of defects in metals is considered.

---

\*This work was supported by the U.S. Department of Energy.

## I. INTRODUCTION

The study of defects in metals has flourished for more than thirty years<sup>1-7</sup> with the frequent introduction of a variety of useful new experimental techniques for the characterization and investigation of lattice defects. These have included electrical resistometry, anelastic measurements, transmission electron microscopy (TEM), differential dilatometry, radiotracer diffusion, nuclear magnetic resonance (NMR), diffuse x-ray scattering, field ion microscopy (FIM), ion channeling, positron annihilation spectroscopy (PAS), Mössbauer spectroscopy, and perturbed angular correlation (PAC). Some of these techniques have had a broad impact on the field of defects in metals, while others have had a narrower, but nevertheless important, application to these problems. Although the first observations of the sensitivity of positron annihilation to nonequilibrium and equilibrium lattice defects in metals were published eighteen<sup>8</sup> and fifteen<sup>9</sup> years ago, respectively, the impact of PAS on the defects field has really only made itself felt over the past decade,<sup>10,11</sup> as an increasing number of problems in this research area have been addressed and solved. It is now clear that PAS, by virtue of its defect-specific sensitivity to a variety of vacancy-like defects in most metals and its applicability to a rather wide range of defect-related problems in materials science, has taken its rightful place among the more useful research tools of the materials scientist.<sup>12</sup>

The impact of PAS upon the field of defects in metals has been greatest in two areas: (i) the determination of properties of atomic defects, especially those of monovacancies, and (ii) the monitoring and characterization of vacancy-like microstructure development during post-irradiation or post-quench annealing. These studies have been carried out primarily in pure metals, but applications of PAS have also been made in these

areas to alloys, in which defect-solute interactions play an important rôle. Such studies in metals and alloys are useful for a variety of reasons. Two of the most important of these are to be able to understand: (i) the atomic-defect mechanisms responsible for mass transport (diffusion) in metals under conditions of essentially thermodynamic equilibrium over their complete temperature range of application, and (ii) the way in which this mass transport is affected under conditions of energetic-particle (e.g., electron, neutron, ion) irradiation. Under these latter, nonequilibrium conditions, such defect-related phenomena as solute segregation, phase stability, and dimensional stability can be dramatically influenced, often with deleterious effects upon the pertinent physical properties of the material in question. Before discussing the rôle that PAS has played in the study of defects in metals vis-à-vis the other available tools for such investigations, it is useful to first consider some of the extant problems in this research area that the positron annihilation techniques can help to solve in the future.

The atomic-defect mechanisms of self-diffusion in metals have been investigated for many years by a combination of radiotracer diffusion measurements and an array of experimental techniques for the study of vacancy defects. These investigations have rather clearly and convincingly demonstrated that atomic exchange with monovacancies is the dominant mechanism by which atoms undergo transport in metals,<sup>13-15</sup> except as the temperature of the metal approaches melting. At these elevated temperatures, in essentially all metals, as the melting temperature is approached, self-diffusion is increasingly enhanced over that which can be attributed to simple atom-monovacancy exchange.<sup>15</sup> An example of this behavior, in tungsten, is shown in Fig. 1. Evidence exists for some face-centered-cubic (fcc) metals, notably aluminum, platinum, and gold, that this diffusion enhancement is caused by the

presence of an increasing population of divacancies in the equilibrium vacancy ensemble with increasing temperature. Not only are there then more vacancy defects present with which atoms can exchange, but also the divacancy is known to be more mobile than the monovacancy in the fcc structure. On the other hand, in the refractory body-centered-cubic (bcc) metals, such as tungsten and molybdenum, there now appears to be rather convincing evidence that the considerably larger high-temperature diffusion enhancement found in these metals cannot be attributed, at least solely, to the presence of divacancies.<sup>15</sup> The possibility that self-interstitial atoms may contribute significantly to atomic transport in both fcc and bcc metals under essentially equilibrium conditions at high temperatures has been suggested as an alternative or supplemental mechanism for this diffusion enhancement. One important aspect of clarifying this situation is to be able to elucidate the nature of the high-temperature equilibrium vacancy ensemble. PAS has been one of our most valuable tools in determining the formation properties of monovacancies in metals; its application to the defect-specific study of the high-temperature vacancy ensemble appears now to be viable, as will be discussed below in Section II B.

A number of the effects of energetic-particle irradiation upon the microstructure of metals and alloys, and the concomitant changes induced in their physical properties, are quite well known.<sup>20</sup> These effects include: (i) radiation-enhanced diffusion, (ii) radiation-induced segregation of elemental constituents, (iii) void formation leading to swelling, and (iv) radiation-induced instability and spatial redistribution of alloy phases. These defect-related phenomena can sometimes have a rather convoluted relationship to the fundamental physical properties of the atomic defects that control them. Nevertheless, an understanding of the underlying defect properties and

interactions is imperative of these more complex phenomena are to be eventually understood and controlled. Two examples will suffice in the present work to demonstrate the nature of the microstructural effects that can ensue from energetic-particle irradiation and the rôle that PAS might play in providing fundamental information regarding these effects.

Radiation-induced segregation of Si to defect sinks in Ni(Si) alloys, in which the Si is normally in solid solution, is shown in Fig. 2. The defect sinks (i.e., annihilation sites) that are decorated by the resulting  $\text{Ni}_3\text{Si}$  precipitates in this example are the surface, grain boundaries, and dislocation loops, the latter resulting from interstitial precipitation in these Ni-ion irradiated samples. Such radiation-induced solute segregation, which similarly occurs for any energetic-particle irradiation that produces excess mobile defects, results from the coupling of a flux of solute atoms, in this case Si, to the flux of radiation-induced excess defects diffusing to the sinks. This coupling exists by virtue of an interaction between the solute element and an atomic defect. The magnitude of such an effect depends upon a number of defect-related properties, including the degree of defect-solute binding, the defect mobilities, and the defect production rate compared with the equilibrium defect concentrations. Owing to the sensitivity of the positron in most metals to the presence of vacancy defects, and the ability of the positron to distinguish between vacancy- and interstitial-type imperfections, PAS can directly provide much of the needed basic information regarding these defect-related properties pertaining to vacancy defects. Indirectly, by comparison with experiments that do not distinguish between vacancies and interstitials, such as electrical resistometry, PAS investigations can yield fundamental information regarding interstitials as well.

The formation of voids in irradiated metals, and the concomitant dimensional swelling of the material, is caused by the precipitation of the excess vacancies that result from an imbalance in the net annihilation rates at defect sinks (mainly dislocations) of the vacancies and interstitials produced by the energetic-particle irradiation. It is a major and costly problem in the use of metals for fuel cladding in nuclear reactors. The rate and magnitude of void swelling depend upon a variety of defect properties, such as equilibrium vacancy concentrations, vacancy and interstitial mobilities, vacancy-cluster binding energies, defect-solute interactions, etc. The morphologies of the void distributions formed during irradiation are normally investigated using transmission electron microscopy (TEM), since this technique offers the most direct information available regarding the size, density, and distribution of these vacancy clusters, as long as they are above the normal TEM resolution limit ( $>20$  Å in diameter) for voids. An example of the utility of TEM for the observation of void distributions is presented in Fig. 3, in which a dramatic ordering is shown of the normal random distribution of voids in irradiated Nb resulting for oxygen concentrations  $\gtrsim 0.04$  at.%.<sup>21</sup> Although PAS cannot, and has no need to, compete with TEM for such morphological observations, it can contribute to the investigation of the void formation and swelling problem in a number of significant ways. These range from the study of the properties of vacancies in metals and alloys, including their interactions with solute elements and extended defects, to the study of the earliest stages of the vacancy precipitation process itself, for which PAS has unique capabilities. The effects upon this precipitation process resulting from the presence of both substitutional and interstitial solute atoms can also be investigated by PAS.

The present paper will consider primarily the investigation of vacancy formation, migration, and clustering by PAS in comparison with the other available techniques for these defect studies. By means of such comparisons, it is hoped that both the particular strengths and weaknesses of PAS as a method for the study and characterization of defect microstructures will be made clear.

## II. VACANCY FORMATION

The study of vacancy formation in metals has been actively pursued for more than 20 years using differential dilatometry, quenching, and, more recently, positron annihilation spectroscopy techniques.<sup>22</sup> Differential dilatometry is based upon the measurement of the relative macroscopic length change ( $\Delta L/L$ ) and microscopic lattice-parameter change ( $\Delta a/a$ ) in a crystal. These measurements, which are normally carried out as a function of temperature under conditions of thermodynamic equilibrium, have the virtue of being rather straightforward in that they yield a value for the total vacancy concentration at each temperature by means of the relation  $C_v = 3 [(\Delta L/L) - (\Delta a/a)]$ , which pertains for an isotropic (i.e., cubic) metal. For anisotropic (e.g., hexagonal) metals, length and lattice-parameter changes along each unique lattice direction must be measured. The practical drawback to differential dilatometry is the precision with which the ( $\Delta a/a$ ) measurements can presently be performed, usually to no better than 5 parts in  $10^5$ . Thus, the technique is limited to measurements of  $C_v > 5 \times 10^{-5}$ . For most metals this is a rather severe limitation, since vacancy concentrations at the melting temperature,  $T_M$ , are of order of magnitude  $10^{-4}$  to  $10^{-3}$ . Thus, either a sufficiently wide temperature and vacancy-concentration range is unavailable to allow for the precise determination of vacancy formation enthalpies (See Fig. 4) or, if the vacancy concentration at  $T_M$  is high, the likelihood of

contributions to the measurements from higher-order vacancy clusters (principally divacancies) cannot be ignored.

#### A. Monovacancies

The results of differential dilatometry measurements of  $C_v$  in copper<sup>23</sup> are shown in Fig. 4, along with the results from two quenching studies.<sup>24,25</sup> These latter, nonequilibrium measurements of the residual resistivity increments (at 4.2 K) from quenched-in vacancies have avoided one of the most problematic pitfalls of quenching investigations of vacancy formation,<sup>26</sup> that of the loss of vacancies to existing sinks (primarily dislocations) during the rapid quench from high temperatures. This has been accomplished by starting with very low dislocation density single crystals<sup>24</sup> or by quenching from sufficiently low temperatures that this loss can be shown to be negligible.<sup>25</sup> The results of these differential dilatometry and quenching studies together are seen to provide a rather consistent description of vacancy formation in copper, as they have in two other fcc metals, aluminum<sup>22</sup> and gold.<sup>26,27</sup> In the case of copper (Fig. 4) these data give no indication of an enhancement in  $C_v$  at high temperatures from the presence of divacancies in the equilibrium vacancy ensemble, whereas for aluminum and gold such an enhancement is clearly evident.<sup>22</sup> However, the problems with performing reliable quenching experiments are considerable, and relating the nonequilibrium quenched-in vacancy ensemble back to the equilibrium vacancy ensemble of interest in these vacancy formation studies is difficult at best.

PAS has provided a means, for the first time, to study vacancy formation in metals under equilibrium conditions with sufficient sensitivity to monitor the changing concentration of vacancies with temperature over the range in which monovacancies dominate the equilibrium vacancy ensemble. This is a

result of the positron being sensitive to vacancy concentration changes in the range of  $<10^{-6}$  to  $10^{-4}$  in most metals. Measurements of the monovacancy formation enthalpy, such as that shown in Fig. 5 for copper,<sup>28</sup> have resulted for a wide variety of metals.<sup>29</sup> These are very often the most precise values for  $H_{1v}^F$  available; however, they do agree well with those obtained from careful quenching studies, when available. A comparison of  $H_{1v}^F$  values obtained from PAS and quenching studies is presented in Table 1 for a few selected fcc and refractory bcc metals.

### B. Divacancies

Self-diffusion in metals is generally observed to be enhanced at high temperatures over that expected from atomic exchange with monovacancies,<sup>15</sup> an effect usually attributed<sup>13,40</sup> to the presence of significant concentrations of divacancies in the equilibrium vacancy ensemble. As a result, PAS data such as those shown in Fig. 5 have also been analyzed for evidence of contributions from these higher-order vacancy clusters. Such attempts at deducing information regarding divacancies, however, yield results that appear to lack uniqueness. The Doppler-broadening data for copper shown in Fig. 5 were analyzed in detail by fitting to a trapping model containing monovacancies alone (1v), or in combination with increasing concentrations of divacancies (1v-2v).<sup>28</sup> It was concluded that no unique information regarding the presence of divacancies in the equilibrium vacancy ensemble could be obtained from this type of positron annihilation data using parametric trapping-model fits. This may be a particularly difficult problem for copper, which has a rather low vacancy concentration at  $T_M$  and for which the data shown in Fig. 4 give no evidence for an enhanced divacancy concentration at high temperatures. The difficulty in obtaining information regarding divacancies from such data as shown in Fig. 5 results from a lack of knowledge

regarding the temperature-dependent annihilation characteristics for the monovacancy- and divacancy-trapped positrons, and hence, a lack of knowledge regarding the limiting high-temperature behavior,  $F_v(T)$ , of the sigmoidal curve. Fortunately, the application of PAS to the problem of the high-temperature equilibrium vacancy ensemble in metals is not limited to such measurements. Two aspects of PAS, one experimental and one theoretical, seem to have now matured to the point where it appears that a successful approach to this problem is at hand.

The full momentum-density information available from two-dimensional angular correlation of annihilation radiation (2D-ACAR), previously used for electronic structure investigations of defect-free metals,<sup>41</sup> can be used for the study of positrons annihilating from vacancy-defect-trapped states within the high-temperature equilibrium vacancy ensemble. In addition, it is now possible to make realistic theoretical calculations of the positron-annihilation characteristics from monovacancy- and divacancy-trapped states in a metal, based upon a self-consistent, local density functional formalism<sup>42</sup> incorporating many-body enhancement effects and carried out for vacancy defects within a supercell.<sup>43</sup> An investigation of the equilibrium vacancy ensemble in aluminum using a combination of these 2D-ACAR experimental and theoretical PAS techniques has very recently been performed,<sup>44</sup> and is described schematically in Fig. 6. The 2D-ACAR surfaces measured in single-crystal aluminum at 20°C, 500°C, and 630°C are shown in Fig. 6. These are referred to a set of 1D-ACAR peak-count measurements as a function of temperature, by means of which the fraction of trapped positrons contributing to the high-temperature 2D-ACAR data could be ascertained. The theoretically calculated 2D-ACAR spectra for positrons annihilating from the Bloch state and the monovacancy- and divacancy-trapped states, to which the data have been

compared, are also presented. The Bloch-state calculation<sup>42</sup> agrees well with the experimentally measured surface at 20°C; the surfaces measured at 500°C and 630°C are observed to lie between the theoretical spectra for the monovacancy- and divacancy-trapped states in terms of both their shape and magnitude.

The preliminary reports<sup>44</sup> of this study are quite encouraging, in that they indicate that these combined experimental and theoretical results are consistent with a significant population of divacancies in the equilibrium vacancy ensemble, which increases with increasing temperature. Such behavior of the equilibrium vacancy ensemble in aluminum is to be expected<sup>22</sup> from a combination of vacancy formation studies using differential dilatometry, quenching, and PAS, as well as post-quench resistivity annealing studies.<sup>31,45</sup> Aluminum, which has a total vacancy concentration at  $T_M$  of  $9.4 \times 10^{-4}$ , is thought to have<sup>22</sup> about 40% of its vacant lattice sites in the form of divacancies at  $T_M$ , about 20% at 500°C, and an almost negligible amount at 300°C. In addition, the presence of divacancies in the high-temperature ensemble is consistent with the rather strong diffusion enhancement observed at high temperatures in aluminum.<sup>13-15</sup> Nevertheless, a unique "fingerprint" of the divacancy has not yet been found in this 2D-ACAR study,<sup>44</sup> although a full analysis of the data has not yet been completed. A number of temperature-dependent effects must still be incorporated into the theoretical calculations, in order to take full advantage of these data. While this initial 2D-ACAR PAS study of an equilibrium vacancy ensemble has been carried out for aluminum, owing to the previously available vacancy-defect information regarding divacancies, neither the experimental nor theoretical techniques used in this study are limited to this simple metal; the techniques can be applied to any metal, even the refractory bcc metals. It is anticipated that

such 2D-ACAR investigations, combining both theory and experiment, will allow for defect-specific, spectroscopic observations of the equilibrium vacancy ensembles in a variety of metals in the future, which can answer a number of important questions regarding their defect-related behavior. Furthermore, it may be expected that such observations can be extended to the study of vacancy-solute interactions in dilute alloys as well, to yield information regarding the change in the electronic structure of a vacancy when it is bound to an impurity. This, of course, is the fundamental information required to understand vacancy-solute interactions in general.

#### C. Vacancy-solute interactions

Studies of vacancy-solute interactions in dilute alloys have been carried out using the same techniques that have been usefully applied to the study of vacancy formation in pure metals, differential dilatometry, quenching, and PAS.<sup>46</sup> Generally, the measurements performed under equilibrium conditions, either using differential dilatometry or PAS, have indicated rather small interactions between substitutional impurities and vacancies; these results are also consistent with radiotracer measurements of solute diffusion in metals.<sup>6</sup> On the other hand, the nonequilibrium, quenching measurements of vacancy-solute interactions have often indicated considerably larger effects.<sup>4</sup> Although the complexity of the defect ensembles in these quenched dilute alloys sometimes precludes a clear analysis, these effects may often be attributable to the stronger interactions among higher-order vacancy and solute clusters, which would not be found to any significant degree in the equilibrium defect ensemble. As in the case of vacancy formation in pure metals, the equilibrium techniques for investigating vacancy-solute interactions are to be preferred.

Since the relative effect on the vacancy concentration enhancement from the presence of vacancy-solute bound states in the equilibrium vacancy ensemble is greatest at lower temperatures,<sup>11</sup> and since any contributions from higher-order vacancy clusters are minimized at such temperatures, PAS measurements of equilibrium vacancy formation in dilute alloys have significant advantages over other available techniques for the study of vacancy-solute interactions in metals. An example of such a measurement<sup>47,48</sup> in Ni(1 at.% Ge) is shown in Fig. 7. Radiation-induced Ge solute segregation has been observed in Ni(Ge) alloys, as in the example shown for Ni(Si) in the Introduction (Fig. 2), and attributed to rather strong vacancy-Ge binding.<sup>49</sup> However, the recent PAS measurements of vacancy formation in Ni(Ge) alloys with various Ge concentrations indicate that this binding enthalpy is only  $0.25 \pm 0.09$  eV.<sup>48</sup> This value is rather small in comparison with the monovacancy formation enthalpy of 1.8 eV in pure Ni,<sup>35</sup> but nevertheless may still be sufficiently large to explain the experimentally observed solute-segregation in these alloys.

Even though PAS measurements have definite advantages over other techniques for these investigations, the results presented in Fig. 7 give a good indication of the difficulty of determining vacancy-solute binding enthalpies using such PAS data. The solute enhancement in the equilibrium vacancy concentration is generally quite small in the case of substitutional solute elements and the positron-annihilation parameter measurements must have sufficient precision to distinguish these small changes. However, the maximum effect from the solute-bound vacancies as seen by the positron, shown in Fig. 7b, is well suited to such measurements. A problem that does have to be given due consideration in these PAS measurements, even more so than for pure metals, is that of positron trapping in dislocations in the pre-vacancy

region.<sup>50</sup> This effect, which can be more of a problem in alloys owing to the additional difficulty in the annealing of solute-, inned dislocations, can lead to an erroneous extrapolation of the low-temperature behavior of the lineshape parameter into the vacancy region and, hence, a deduced vacancy-solute binding enthalpy that is larger than that in reality.<sup>48</sup> Nevertheless, carefully performed PAS investigations of vacancy formation in dilute alloys, and in concentrated alloys as well, can provide much needed fundamental information regarding the defect-related behavior of such materials.

### III. VACANCY MIGRATION

The study of vacancy migration in metals has been fruitfully attacked along two paths, which have most often, but not always, yielded results consistent with one another. One path has been the essentially direct measurement of vacancy mobility by monitoring the temperature-dependent annealing of a nonequilibrium ensemble of vacancies introduced into the metal by quenching or energetic-particle (preferably electron) irradiation.<sup>51</sup> The other path has been the more indirect, but often preferable one, of combining the results of monovacancy formation and low-temperature radiotracer diffusion studies to deduce monovacancy migration enthalpies.<sup>13,22</sup> As long as the non-equilibrium defect ensemble introduced into the metal by quenching or irradiation is not too complex, as it most often is in the cases of heavy-particle (neutron,ion) irradiation or mechanical deformation, this annealing can be interpreted in terms of the mobilities of the individual defects comprising the ensemble.<sup>52</sup> The experimental techniques used to monitor this annealing behavior have been diverse, including almost all of those mentioned at the outset of this paper. Positron annihilation has found its niche in both of these methods to deduce the migration properties of vacancy defects.

Since the activation enthalpy for self-diffusion by atomic exchange with monovacancies is given by  $Q_1 = H_{1v}^F + H_{1v}^M$ , precise measurements of  $Q_1$  by radiotracer diffusion or nuclear magnetic resonance methods can be combined with similarly precise measurements of  $H_{1v}^F$  to yield values for the monovacancy migration enthalpy,  $H_{1v}^M$ . Some examples are presented in Table 1. When the measurements of  $Q_1$  and  $H_{1v}^F$  are straightforward, as for the examples given in Table 1, requiring no ad hoc assumptions in the analysis of either the diffusion or vacancy-formation data, this method for determining  $H_{1v}^M$ , basically under equilibrium conditions and a rather simple defect situation, can yield the most accurate values available for this migration enthalpy. These values also agree well with those available from post-quench and post-irradiation annealing studies.<sup>51</sup> On the other hand, when the determination of either  $Q_1$  or  $H_{1v}^F$ , or both, requires a more complex and model-dependent analysis than usual, as in the case of metals undergoing high-temperature phase transitions<sup>53,54</sup> or when positron detrapping from vacancies is suspected,<sup>37</sup> this method can yield results which are considerably less reliable than those available from the more direct studies of vacancy mobility in quenched or electron-irradiated metals.

PAS has been particularly useful in monitoring vacancy annealing in metals after irradiation or quenching, owing to the rather unique sensitivity of the positron to vacancy defects. Thus, even in a defect ensemble containing both vacancies and interstitials, produced by energetic-particle irradiation, PAS is able to distinguish those temperature regions in which vacancies are mobile and form clusters from those in which vacancy-interstitial recombination occurs. This defect-specific sensitivity of the positron has consequently helped significantly in confirming that mobile vacancies are responsible for what is normally called Stage III annealing in

irradiated metals.<sup>52</sup> A controversy existed for a number of years regarding this annealing stage, owing in part to the lack of defect-specificity of previously used techniques, such as electrical resistometry, which allowed for interpretation of this annealing in terms of either vacancies or interstitials.

An example of the application of the PAS lifetime technique to the direct study<sup>55</sup> of vacancy mobility in electron-irradiated  $\alpha$ Fe is shown in Fig. 8. In this study, the observed post-irradiation annealing of the defect-trapped positron lifetime  $\tau_2$  and the intensity  $I_2$  of this component in the lifetime spectrum clearly indicates that vacancies are mobile at about 220 K in  $\alpha$ Fe. The annealing of  $I_2$  in the low-dose sample at 140 K, along with the absence of any concomitant change in  $\tau_2$  at this temperature, suggests that vacancy-interstitial recombination has occurred in this annealing stage. The annealing of  $I_2$  at 220 K, in both the high- and low-dose irradiated samples, along with the concomitant increase of  $\tau_2$  from that value attributable to monovacancies (about 175 ps) to those values representative of small vacancy clusters,<sup>56,57</sup> show clearly that vacancy precipitation is taking place at this temperature. This direct observation of vacancy mobility at about 220 K in  $\alpha$ Fe is at odds with the indirect deduction of a monovacancy mobility in  $\alpha$ Fe from a combination of equilibrium PAS<sup>54</sup> and radiotracer diffusion<sup>53</sup> results, which suggest that the monovacancy in  $\alpha$ Fe only becomes mobile at considerably higher temperatures. However, this appears to be a good case in point for the greater reliability of the more direct measurement of vacancy mobility by PAS compared with the indirect method for a metal which undergoes multiple high-temperature phase transitions. Recent measurements using a variety of techniques, including PAS, TEM, magnetic after-effect measurements, and electrical resistometry, have confirmed the low-temperature mobility of the vacancy in  $\alpha$ Fe.<sup>56</sup>

Before proceeding to a consideration of vacancy clustering in metals, it may be useful to point out a feature of such direct measurements of vacancy mobility using PAS which has not been taken advantage of, at least up until the present (an exception can be found in these Proceedings<sup>57</sup>). PAS measurements of vacancy mobility in nonequilibrium defect ensembles have concentrated upon determining the temperature range in which vacancies become mobile, qualitatively useful information, but have not heretofore gone beyond this to quantitatively determine a vacancy migration enthalpy, which is necessary input in the modeling of complex defect-related behavior found in real materials. Although more tedious than isochronal annealing studies, as that shown in Fig. 8, isothermal annealing measurements at a variety of temperatures within the defect-mobile region can yield quantitative measurements<sup>52</sup> of the vacancy migration enthalpy by PAS, as they have using electrical resistometry and TEM. Such measurements would be particularly useful, of course, for those metals (e.g.,  $\alpha$ Fe, V, Nb, Ta) in which the comparison of the results of low-temperature diffusion studies and monovacancy formation enthalpy measurements have yielded questionable<sup>58</sup> values for the monovacancy migration enthalpy.<sup>37,54</sup>

#### IV. VACANCY CLUSTERING

Vacancy clustering in metals, leading to the formation of dislocation loops, voids, or bubbles, has been widely studied by TEM, by a combination of electrical resistometry and TEM, and, more recently, by PAS. Diffuse x-ray scattering, FIM, and ion channeling have also been used for such studies, but only in a few selected cases. Reviews of many of these applications can be found in Ref. 12. Transmission electron microscopy has been the technique of choice in most studies of vacancy clustering, since it yields direct information regarding the size, nature, and spatial distribution of the

clusters, with good sampling statistics, if done appropriately. TEM can also yield the relationship between such information and that of other microstructural features of interest in the material (e.g., dislocations, grain boundaries, surfaces). In these areas of microstructural observation, no other technique competes effectively with TEM. The limitations of TEM in performing these tasks are primarily its lack of resolution of very small vacancy clusters ( $\leq 20 \text{ \AA}$ ) and its inability to monitor the earliest stages of the segregation of impurities, either substitutional or interstitial, to these clusters. While FIM can, in principal, owing to its atomic resolution and analytical capabilities,<sup>59</sup> complement TEM in these areas, its sampling statistics are too limited to high-density events for general applicability. Positron annihilation spectroscopy, by virtue of the positron's unique sensitivity to vacancy defects in the complete range from single vacancies to small vacancy clusters to clusters of vacancies large enough to be observed by TEM and its ability to distinguish the chemical environment of these vacancy defects, both with good sampling statistics, can complement TEM investigations of vacancy clusters as no other technique available to the materials scientist can. However, much of this potential is as yet unrealized, although this situation appears to be changing rapidly.<sup>60</sup>

Examples of the application of PAS to the investigation of vacancy clustering in electron<sup>61</sup> and neutron<sup>62</sup> irradiated molybdenum are shown in Fig. 9. The defect-trapped positron lifetime  $\tau_2$  is seen to vary continuously with annealing in the electron-irradiated sample from that value (200 ps) representative of monovacancies in Mo to about 450 ps, which is representative of well defined voids<sup>64</sup> in this material. This observed variation of  $\tau_2$  with post-irradiation annealing temperature led to two subsequent investigations: one,<sup>64</sup> a quantitative analysis of the vacancy clustering process in terms of

calculated positron lifetimes in voids in Mo as a function of void size, the other,<sup>61</sup> within the context of the original investigation, a confirmation of the PAS-observed void formation by means of TEM. The voids observed by TEM were about 30 Å in diameter and at a density of about 1 to  $5 \times 10^{13}$  voids  $\text{cm}^{-3}$ , close to the limits of both the resolution and sampling capabilities of conventional TEM. The ability of PAS to distinguish between differing states of vacancy clustering in samples that have undergone different irradiation conditions is clearly shown by a comparison of the initial post-irradiation states of the vacancies in the electron and neutron irradiated samples as seen by the positron. The larger initial value of  $\tau_2$  in the latter case as compared with the former, distinguishes rather clearly between the void-like nature of the depleted zones present after neutron irradiation and the monovacancies present after electron irradiation, which results in rather simple Frenkel-pair (i.e., vacancy plus interstitial) production.

The increase in  $\tau_2$  above 450 ps, shown in Fig. 9, observed for both the electron and neutron irradiated molybdenum at annealing temperatures in excess of 600°C was subsequently shown<sup>63</sup> to have been due to impurity contamination of the voids from the gaseous annealing atmosphere. The demonstrated sensitivity of PAS to such an impurity-contamination effect can have considerable impact on the study of the earliest stages of solute segregation to voids and its eventual influence upon the void formation and swelling problem in alloys. While such applications of PAS have been somewhat slowly realized, it can now be anticipated from several recent studies<sup>60</sup> that PAS investigations of impurity segregation at voids will provide an important complement to the large number of TEM investigations of this technologically important problem, which after all can only observe the later stages of these segregation processes.

It should be pointed out that the study of vacancy clustering, and for that matter vacancy mobility, is in no way limited to the PAS lifetime technique, although these were the examples chosen for Figs. 8 and 9. The PAS momentum techniques, Doppler broadening and angular correlation, can be similarly applied to these problems, with the particular advantage that specific chemical environments related to these defect clusters may be more effectively probed than with lifetime measurements. In order to fully utilize the potential of these momentum measurements, however, defect-specific parameters of the positron annihilation spectra must be developed and calibrated. Such a parameter, for example, has been used effectively in studies of vacancy clustering in copper and hydrogen-doped copper.<sup>65-67</sup> With the recent advent of realistic calculations of the positron-annihilation parameters in defect-trapped states,<sup>42,44,68</sup> it can be anticipated that the PAS momentum techniques will become much more powerful tools for these applications to vacancy clustering phenomena in the near future.

#### V. CONCLUSIONS

This paper has focused upon the investigation of vacancy formation, vacancy migration, and vacancy clustering in metals by PAS in comparison with other experimental techniques available for such studies. These areas of application within the field of defects in metals were selected since they represent the areas in which PAS has made the most significant contributions to date and in which it will likely do so in the relatively near future. Positron annihilation studies of deformed metals and alloys have also been carried out, and the sensitivity of the positron to the defect microstructures thus produced have been clearly demonstrated. Unfortunately, at this time there is an insufficient understanding of the way in which the positron interacts competitively with the variety of potential positron trap states in

the rather complex defect ensembles produced by mechanical deformation. Much the same thing might be said at present regarding the application of PAS to complex irradiation-induced defect ensembles. While PAS can indeed be very useful in qualitatively monitoring the gross changes which may occur in such complex defect ensembles, it is unlikely that much defect-specific information can be deduced from these changes until the response of the positron to a number of possible defect-trap states can be elucidated.

For example, the response of positrons to trapping in dislocation lines vis-à-vis jogs along these dislocation lines has been considered theoretically.<sup>69</sup> It has been suggested that weak positron trapping at the dislocation, in conjunction with stronger trapping at jog sites, may explain a number of the prevacancy effects observed even in supposedly well-annealed metals,<sup>50</sup> which of course always contain some residual dislocations. While this suggestion seems to account for many of these observations, a clear experimental demonstration of the differing positron trapping and annihilation response to dislocation lines and jogs along these lines is still lacking. The realistic interpretation of PAS data in deformed metals would naturally depend rather heavily on the clarification of this problem. Similar questions remain in terms of the positron's response to other extended defects in metals, such as grain boundaries, and interfaces between phases in alloys. Careful investigations by PAS of previously characterized microstructures, for example, by TEM, would be exceedingly valuable in this regard.

Whether PAS will become as valuable a technique for the study of more complex defect-related behavior in metals and alloys as it has been for the study of the properties of vacancies, is a question that remains to be answered. There appear, however, to be rather few a priori limitations to the application of PAS to the study of defects in metals and alloys, either by

itself or as a complement to other available experimental techniques. These applications will undoubtedly be given even a broader scope with the recent availability of slow positron beam sources with positron acceleration capabilities.<sup>70,71</sup> These positron sources can be used to probe near-surface defects in a depth-dependent fashion, and possibly laterally-dispersed defects, as well, using focused positron beams, in the future. A major factor in determining how far PAS can be eventually taken in its effective applicability to the study of defects in metals may well be the degree to which realistic theoretical calculations of positron response to various defect types can be carried practically. Just as transmission electron microscopy has relied upon calculations of the expected diffraction contrast from various defects for its most sophisticated applications to the observation of defect microstructures, so positron annihilation spectroscopy may ultimately depend upon a combination of theory and experiment for a utilization of its full potential for the study of defects in metals. At this writing, the future of these applications of PAS looks bright indeed.

## REFERENCES:

1. W. Shockley, J. H. Hollomon, R. Maurer, and F. Seitz, eds., Imperfections in Nearly Perfect Crystals (Wiley, New York, 1952).
2. Defects in Crystalline Solids, Report of the Bristol Conference (The Physical Society, London, 1955).
3. D. S. Billington, ed., Radiation Damage in Solids (Academic, New York, 1962).
4. R. M. J. Cotterill, M. Doyama, J. J. Jackson, and M. Meshii, eds., Lattice Defects in Quenched Metals (Academic, New York, 1965).
5. A. Seeger, D. Schumacher, W. Schilling, and J. Diehl, eds., Vacancies and Interstitials in Metals (North-Holland, Amsterdam, 1970).
6. N. L. Peterson and R. W. Siegel, eds., Properties of Atomic Defects in Metals (North-Holland, Amsterdam, 1978); J. Nucl. Mater. 69 & 70 (1978).
7. J. Takamura, M. Doyama, and M. Kiritani, eds., Point Defects and Defect Interactions in Metals (University of Tokyo, Tokyo, 1982).
8. I. Ya. Dekhtyar, D. A. Levina, and V. S. Mikhalev, Soviet Physics-Doklady 9, 492 (1964).
9. I. K. MacKenzie, T. L. Khoo, A. B. McDonald, and B. T. A. McKee, Phys. Rev. Lett. 19, 946 (1967).
10. A. Seeger, J. Phys. F: Metal Phys. 3, 248 (1973).
11. M. Doyama and R. R. Masiguti, Crystal Lattice Defects 4, 139 (1973).
12. F. W. Wiffen and J. A. Spitznagel, eds., Advanced Techniques for Characterizing Microstructures (The Metallurgical Society of AIME, Warrendale, Pennsylvania, 1982); R. W. Siegel, in Ref. 12, p. 413.
13. A. Seeger and H. Mehrer, in Ref. 5, p. 1.
14. N. L. Peterson, in Ref. 6, p. 3.
15. R. W. Siegel, in Ref. 7, in press.

16. J. N. Mundy, S. J. Rothman, N. Q. Lam, H. A. Hoff, and L. J. Nowicki, Phys. Rev. B 18, 6566 (1978).
17. N. K. Arkhipova, S. M. Klotzman, Y. A. Robovskii, and A. N. Timofeyev, Fiz. Met. Metalloved. 43, 779 (1977).
18. R. E. Pawel and T. S. Lundy, Acta Metall. 17, 979 (1969).
19. R. L. Andelin, J. D. Knight, and M. Kahn, Trans. Metall. Soc. AIME 233, 19 (1965).
20. H. Wiedersich, in Ref. 12, p. 15.
21. B. A. Loomis and S. B. Gerber, J. Nucl. Mater. 97, 113 (1981).
22. R. W. Siegel, in Ref. 6, p. 117.
23. R. O. Simmons and R. W. Balluffi, Phys. Rev. 129, 1533 (1963).
24. R. R. Bourassa and B. Lengeler, J. Phys. F: Metal Phys. 6, 1405 (1976).
25. A. S. Berger, S. T. Ockers, and R. W. Siegel, J. Phys. F: Metal Phys. 9, 1023 (1979).
26. R. W. Balluffi, K. H. Lie, D. N. Seidman, and R. W. Siegel, in Ref. 5, p. 125.
27. R. P. Sahu, K. C. Jain, and R. W. Siegel, in Ref. 6, p. 264.
28. M. J. Fluss, L. C. Smedskjaer, R. W. Siegel, D. G. Legnini, and M. K. Chason, J. Phys. F: Metal Phys. 10, 1763 (1980).
29. R. N. West, in Positrons in Solids, P. Hautojärvi, ed., (Springer, Berlin, 1979) p. 89.
30. M. J. Fluss, L. C. Smedskjaer, M. K. Chason, D. G. Legnini, and R. W. Siegel, Phys. Rev. B 17, 3444 (1978).
31. A. S. Berger, S. T. Ockers, M. K. Chason, and R. W. Siegel, in Ref. 6, p. 734.
32. Y. C. Jean, K. G. Lynn, and J. E. Dickman, Phys. Rev. B 21, 2655 (1980).
33. M. Doyama and J. S. Kochler, Phys. Rev. 127, 21 (1962).

34. W. Triftshäuser and J. D. McGervey, *Appl. Phys.* 6, 177 (1975).
35. L. C. Smedskjaer, M. J. Fluss, D. G. Legnini, M. K. Chason, and R. W. Siegel, *J. Phys. F: Metal Phys.* 11, 2221 (1981).
36. W. Wycisk and M. Feller-Kniepmeier, *phys. stat. sol. (a)* 37, 183 (1976).
37. K. Maier, M. Peo, B. Saile, H. E. Schaefer, and A. Seeger, *Phil. Mag. A* 40, 701 (1979).
38. I. A. Schwirtlich and H. Schultz, *Phil. Mag. A* 42, 601 (1980).
39. K.-D. Rasch, R. W. Siegel, and H. Schultz, *Phil. Mag. A* 41, 91 (1980);  $H_{1v}^F$  from data of Fig. 6, Ref. 39 using a revised  $\rho(T)$  scale from J. N. Mundy, *Phil. Mag. A*, in press (1982).
40. N. L. Peterson, *Comments in Solid State Phys.*, 8, 107 (1978).
41. S. Berko, M. Raghooie, and J. J. Mader, *Phys. Lett.* 63A, 335 (1977); see also, S. Berko, in Positron Annihilation, R. R. Hasiguti and K. Fujiwara, eds., (The Japan Institute of Metals, Sendai, 1979) p. 65.
42. B. Chakraborty, *Phys. Rev. B* 24, 7423 (1981); see also, these Proceedings.
43. R. P. Gupta and R. W. Siegel, *Phys. Rev. Lett.* 39, 1212 (1977); *Phys. Rev. B* 22, 4572 (1980).
44. M. J. Fluss, S. Berko, B. Chakraborty, K. Hoffmann, P. Lippel, and R. W. Siegel, *Proc. Sixth Intl. Conf. on Positron Annihilation*, P. G. Coleman, S. C. Sharma, and L. M. Diana, eds. (North-Holland, Amsterdam, 1982) in press; see also, B. Chakraborty, S. Berko, M. J. Fluss, K. Hoffman, P. Lippel, and R. W. Siegel, these Proceedings.
45. V. Levy, J. M. Lanore, and J. Hillairet, *Phil. Mag.* 28, 373 (1973).
46. M. Doyama, in Ref. 6, p. 350.
47. L. C. Smedskjaer, M. J. Fluss, D. G. Legnini, M. K. Chason, and R. W. Siegel, in Ref. 7, in press.

48. L. C. Smedskjaer, M. J. Fluss, D. G. Legnini, M. K. Chason, and R. W. Siegel, Proc. Sixth Intl. Conf. on Positron Annihilation, P. G. Coleman, S. C. Sharma, and L. M. Diana, eds. (North-Holland, Amsterdam, 1982) in press.
49. R. P. Gupta and N. Q. Lam, Scripta Metall. 13, 1005 (1979).
50. L. C. Smedskjaer, Proc. Sixth Intl. Conf. on Positron Annihilation, P. G. Coleman, S. C. Sharma, and L. M. Diana, eds. (North-Holland, Amsterdam, 1982) in press.
51. R. W. Balluffi, in Ref. 6, p. 240.
52. R. W. Balluffi and R. W. Siegel, in Ref. 4, p. 693.
53. G. Hettich, H. Mehrer, and K. Maier, Scripta Metall. 11, 795 (1977).
54. H.-E. Schaefer, K. Maier, M. Weller, D. Herlach, A. Seeger, and J. Diehl, Scripta Metall. 11, 803 (1977).
55. P. Hautojärvi, T. Judin, A. Vehanen, J. Yli-Kauppila, J. Johansson, J. Verdone, and P. Moser, Solid State Commun. 29, 855 (1979).
56. P. Hautojärvi, Proc. Sixth Intl. Conf. on Positron Annihilation, P. G. Coleman, S. C. Sharma, and L. M. Diana, eds. (North-Holland, Amsterdam, 1982) in press.
57. C. S. Sundar, A. Bharathi, S. K. Sarkar, G. Amarendra, and K. P. Gopinathan, these Proceedings.
58. H. Schultz, in Ref. 7, in press.
59. A. Wagner, T. M. Hall, and D. N. Seidman, in Ref. 6, p. 413.
60. P. G. Coleman, S. C. Sharma, and L. M. Diana, eds., Proc. Sixth Intl. Conf. on Positron Annihilation (North-Holland, Amsterdam, 1982) in press.
61. M. Eldrup, O. E. Mogensen, and J. H. Evans, J. Phys. F: Metal Phys. 6, 499 (1976).
62. K. Petersen, N. Thrane, and R. M. J. Cotterill, Phil. Mag. 29, 9 (1974).

63. N. Thrane and J. H. Evans, Proc. Fourth Intl. Conf. on Positron Annihilation, Helsingør, Denmark, 1976, part 2, E19, p. 100, unpublished.
64. P. Hautojärvi, J. Heiniö, M. Manninen, and R. Nieminen, Phil. Mag. 35, 973 (1977).
65. S. Mantl and W. Triftshäuser, Phys. Rev. Lett. 34, 1554 (1975).
66. S. Mantl and W. Triftshäuser, Phys. Rev. B 17, 1645 (1978).
67. B. Lengeler, S. Mantl, and W. Triftshäuser, J. Phys. F: Metal Phys. 8, 1691 (1978).
68. M. J. Puska and R. M. Nieminen, J. Phys. F: Metal Phys. 12, in press (1982); see also, R. M. Nieminen and M. J. Puska, in Ref. 60, in press.
69. L. C. Smedskjaer, M. Manninen, and M. J. Fluss, J. Phys. F: Metal Phys. 10, 2237 (1980).
70. K. G. Lynn, Phys. Rev. Lett. 44, 1330 (1980).
71. W. Triftshäuser and G. Kügel, in Ref. 60, in press.

Table 1. Monovacancy formation enthalpies,  $H_{1v}^F$ , from PAS compared with those from quenching. The 'best' values for  $H_{1v}^F$  are subtracted from the activation enthalpies for low-temperature diffusion,  $Q_1$ , to yield values for the monovacancy migration enthalpy,  $H_{1v}^M$ .<sup>15</sup>

Metal	$H_{1v}^F$ (eV)		$Q_1$ (eV)	$H_{1v}^M$ (eV)
	PAS	Quenching		
Al	$0.66 \pm 0.02$ <sup>30</sup>	$0.66 \pm 0.01$ <sup>31</sup>	0.66	1.28
Ag	$1.11 \pm 0.05$ <sup>32</sup>	$1.10$ <sup>33</sup>	1.11	1.76
Au	$0.97 \pm 0.01$ <sup>34</sup>	$0.94 \pm 0.02$ <sup>27</sup>	0.94	1.78
Cu	$1.31 \pm 0.05$ <sup>28</sup>	$1.30 \pm 0.05$ <sup>25</sup>	1.31	2.07
Ni	$1.8 \pm 0.1$ <sup>35</sup>	$1.6$ <sup>36</sup>	1.8	2.88
Mo	$3.0 \pm 0.2$ <sup>37</sup>	$3.2$ <sup>38</sup>	3.2	4.5
W	$4.0 \pm 0.3$ <sup>37</sup>	$3.6 \pm 0.2$ <sup>39</sup>	3.6	5.4

## FIGURE CAPTIONS

Fig. 1. Self-diffusion in tungsten; logarithm of the tracer self-diffusion coefficient as a function of reciprocal temperature.<sup>16-19</sup> The expected behavior from atomic exchange with monovacancies,  $D_{1v}$ , is indicated, as are the low- and high-temperature activation enthalpies,  $Q_1$  and  $Q_2$ , respectively.<sup>16</sup>

Fig. 2. Radiation-induced solute segregation in normally solid solution Ni(Si) alloys, leading to  $Ni_3Si$  precipitation observable by TEM at such defect sinks as: (a) the surface, (b) interstitial dislocation loops, and (c) a grain boundary. After R. f. 20.

Fig. 3. Transmission electron micrographs of void distributions in Nb containing (a) 0.004 at.% O or (b) 0.039 at.% O after Ni-ion irradiation at 1050 K. From Ref. 21.

Fig. 4. The total equilibrium vacancy concentration in copper; logarithm of  $C_v$  as a function of reciprocal temperature. The post-quench resistivity data<sup>24,25</sup> are scaled to the  $C_v$  values measured by differential dilatometry<sup>23</sup> using a vacancy resistivity of  $0.62 \times 10^{-4} \Omega \text{ cm}$ . After Ref. 25.

Fig. 5. Doppler-broadening lineshape parameter  $F(T)$  for copper as a function of temperature, and four statistically indistinguishable trapping-model fits to the data.<sup>28</sup> The  $F_v(T)$  deduced from these fits (1v or 1v-2v) are seen to accommodate to the uncertainties regarding the high-temperature vacancy ensemble.

Fig. 6. Schematic of a 2D-ACAR investigation of the equilibrium vacancy ensemble in aluminum.<sup>44</sup> The experimental 2D-ACAR surfaces for an Al single crystal at 20°C, 500°C, and 630°C, measured at Brandeis University, are compared with the theoretical 2D-ACAR spectra, calculated for 0 K and convoluted with the experimental resolution, for the Bloch state and the monovacancy (1v) and divacancy (2v) trapped states of the positron. The  $p_z$  and  $p_y$  axes correspond to <110> directions for the experiment and <100> directions for the theory; the representations are rotated accordingly. The 2D-ACAR data are referred here to a set of measured  $p_z = <111>$ , 1D-ACAR (long-slit) data as a function of temperature for convenience of visualization.

Fig. 7. (a) Doppler-broadening lineshape parameter  $F(T)$  for Ni and Ni(1 at.% Ge) as a function of temperature, and the trapping model fits to these data. From Ref. 47.

(b) The difference  $\Delta F(T)$  between the data for the Ni(1 at.% Ge) and the Ni shown in (a) as a function of temperature. From Ref. 48. This difference has been set to zero at the lowest temperature.

Fig. 8. The lifetime  $\tau_2$  of trapped positrons, and the intensity  $I_2$  of this component, in electron irradiated  $\alpha$ -Fe as a function of annealing temperature. From Ref. 55.

Fig. 9. Annealing behavior of the trapped-positron lifetime  $\tau_2$  in electron<sup>61</sup> and neutron<sup>62</sup> irradiated molybdenum. After Ref. 63.

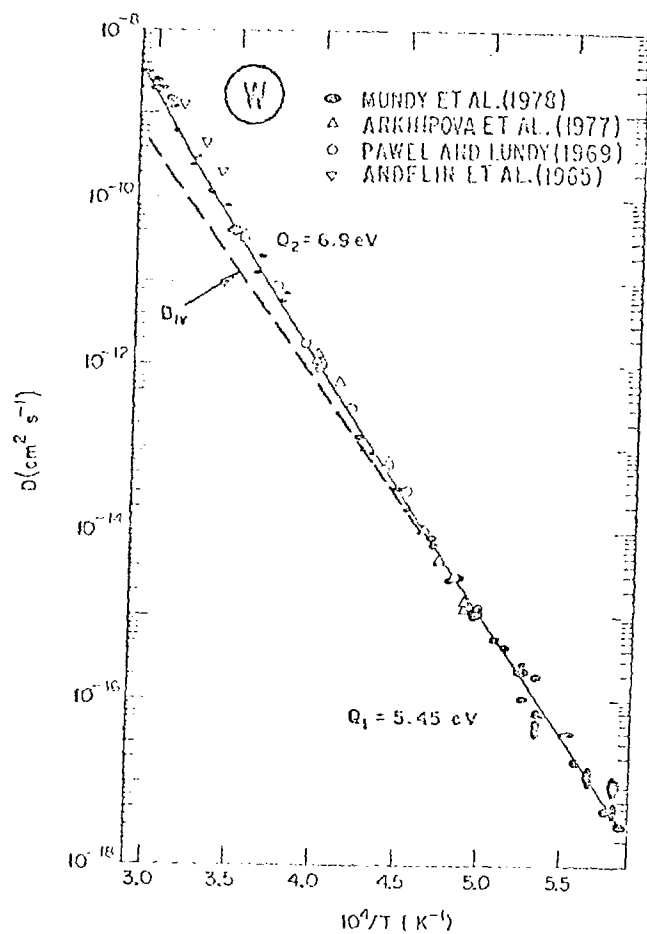


Fig. 1. Self-diffusion in tungsten; logarithm of the tracer self-diffusion coefficient as a function of reciprocal temperature.<sup>16-19</sup> The expected behavior from atomic exchange with monovacancies,  $D_{IV}$ , is indicated, as are the low- and high-temperature activation enthalpies,  $Q_1$  and  $Q_2$ , respectively.<sup>16</sup>

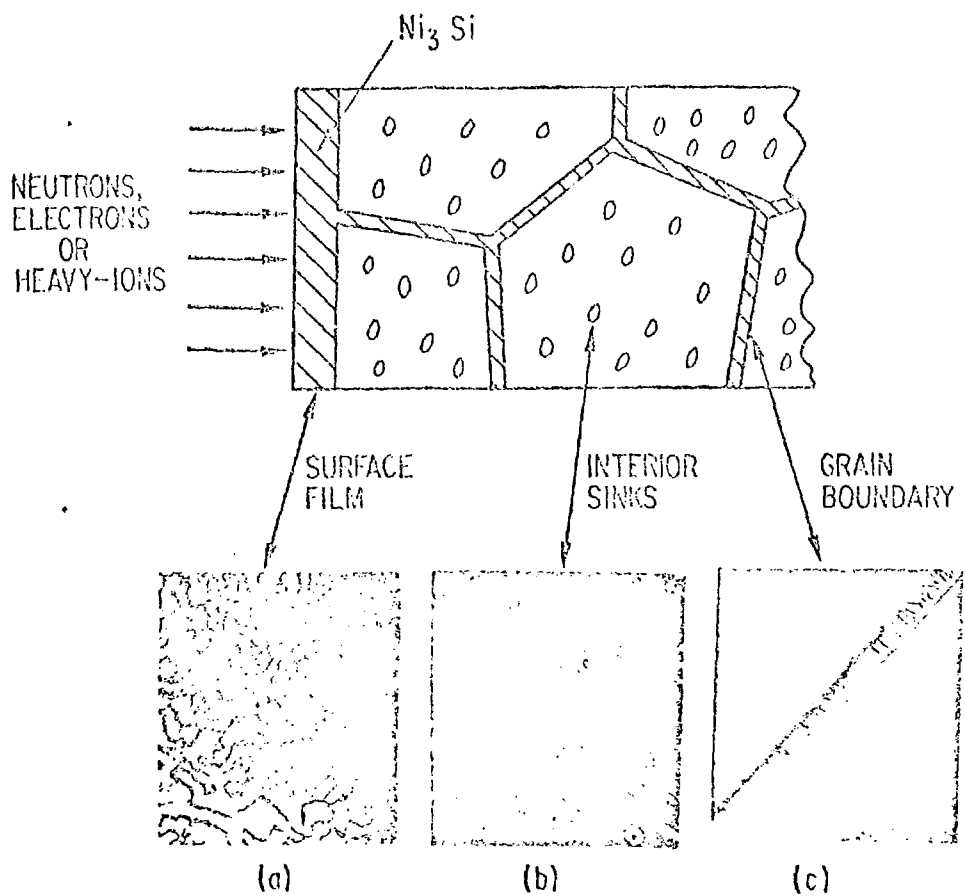


Fig. 2. Radiation-induced solute segregation in normally solid solution  $\text{Ni}(\text{Si})$  alloys, leading to  $\text{Ni}_3\text{Si}$  precipitation observable by TEM at such defect sinks as: (a) the surface, (b) interstitial dislocation loops, and (c) a grain boundary. After Ref. 20.

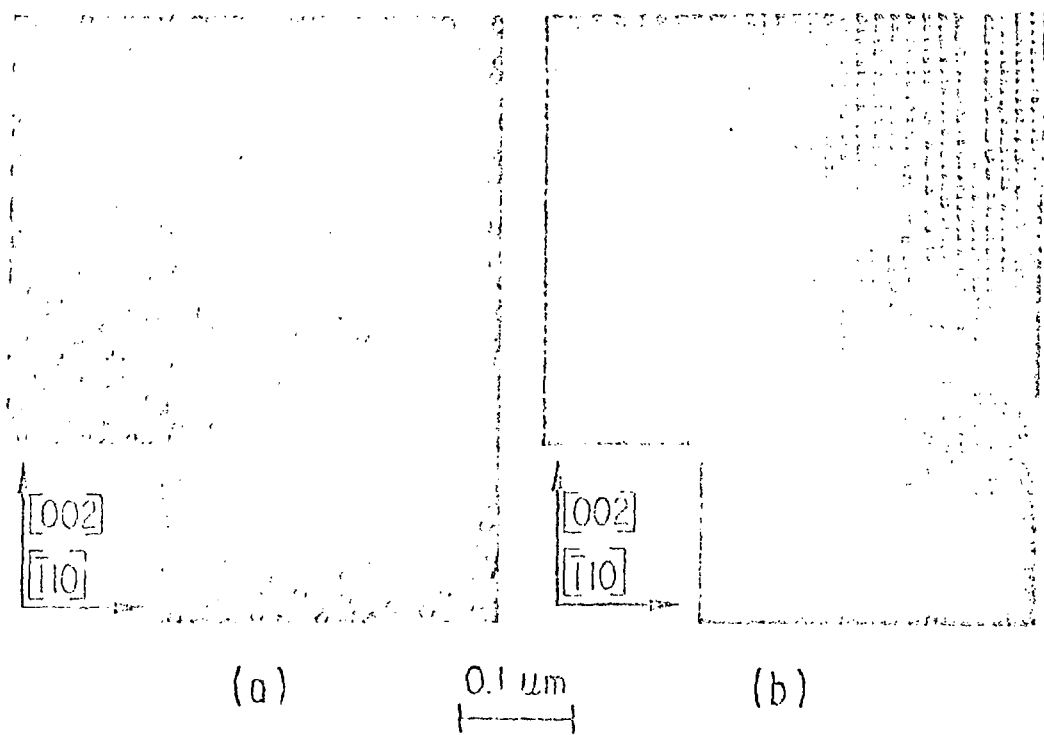


Fig. 3. Transmission electron micrographs of void distributions in Nb containing (a) 0.004 at.% O or (b) 0.039 at.% O after Ni-ion irradiation at 1050 K. From Ref. 21.

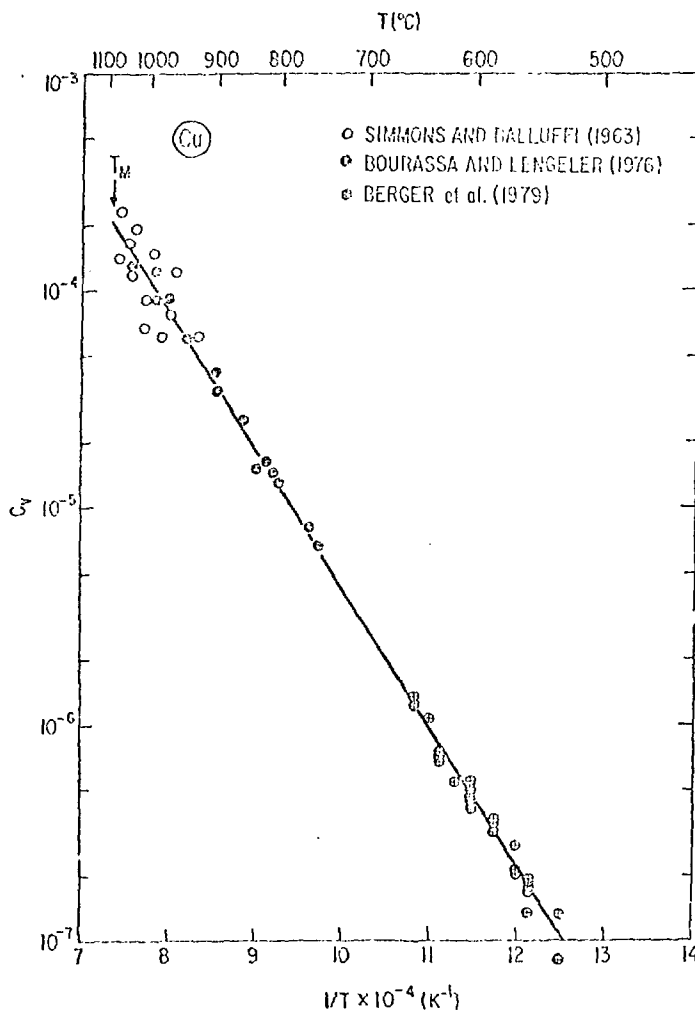


Fig. 4. The total equilibrium vacancy concentration in copper; logarithm of  $C_v$  as a function of reciprocal temperature. The post-quench resistivity data<sup>24,25</sup> are scaled to the  $C_v$  values measured by differential dilatometry<sup>23</sup> using a vacancy resistivity of  $0.62 \times 10^{-4} \Omega \text{ cm}$ . After Ref. 25.

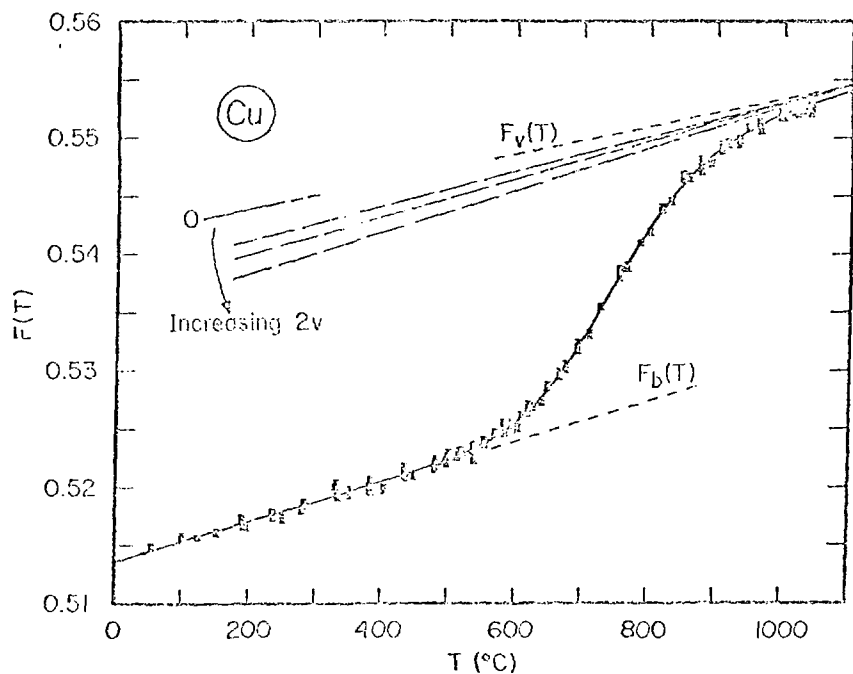


Fig. 5. Doppler-broadening lineshape parameter  $F(T)$  for copper as a function of temperature, and four statistically indistinguishable trapping-model fits to the data.<sup>28</sup> The  $F_v(T)$  deduced from these fits (1v or 1v-2v) are seen to accommodate to the uncertainties regarding the high-temperature vacancy ensemble.

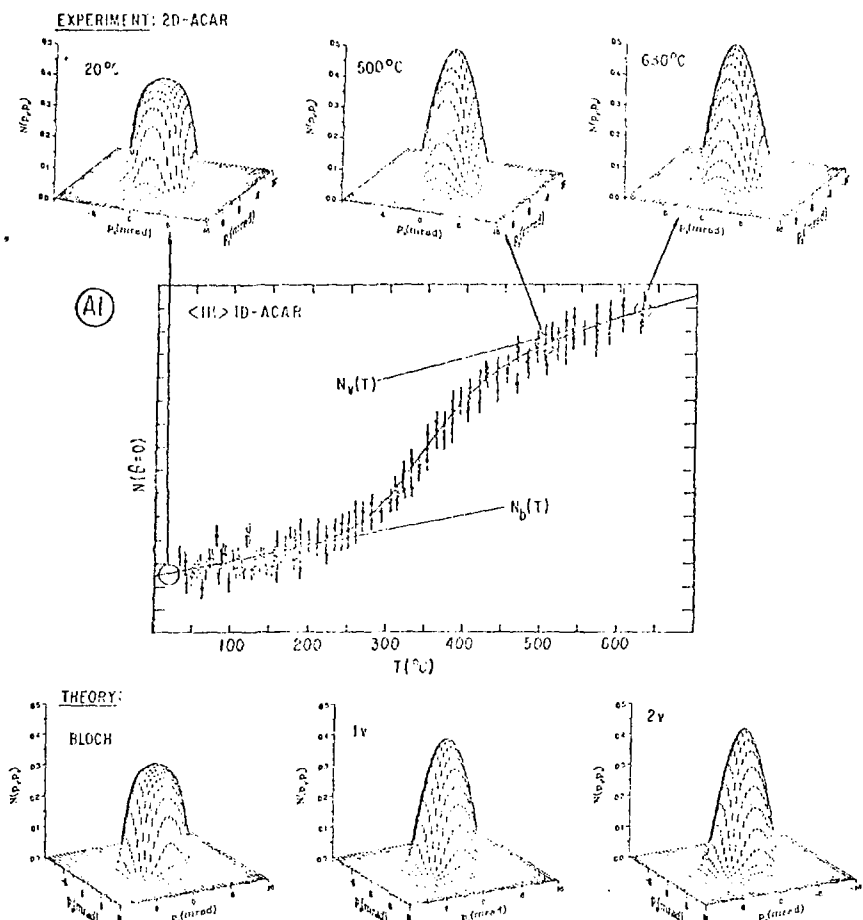


Fig. 6. Schematic of a 2D-ACAR investigation of the equilibrium vacancy ensemble in aluminum.<sup>44</sup> The experimental 2D-ACAR surfaces for an Al single crystal at 20°C, 500°C, and 630°C, measured at Brandeis University, are compared with the theoretical 2D-ACAR spectra, calculated for 0 K and convoluted with the experimental resolution, for the Bloch state and the monovacancy (1v) and divacancy (2v) trapped states of the positron. The  $p_z$  and  $p_y$  axes correspond to  $\langle 110 \rangle$  directions for the experiment and  $\langle 100 \rangle$  directions for the theory; the representations are rotated accordingly. The 2D-ACAR data are referred here to a set of measured  $p_z = \langle 111 \rangle$ , 1D-ACAR (long-slit) data as a function of temperature for convenience of visualization.

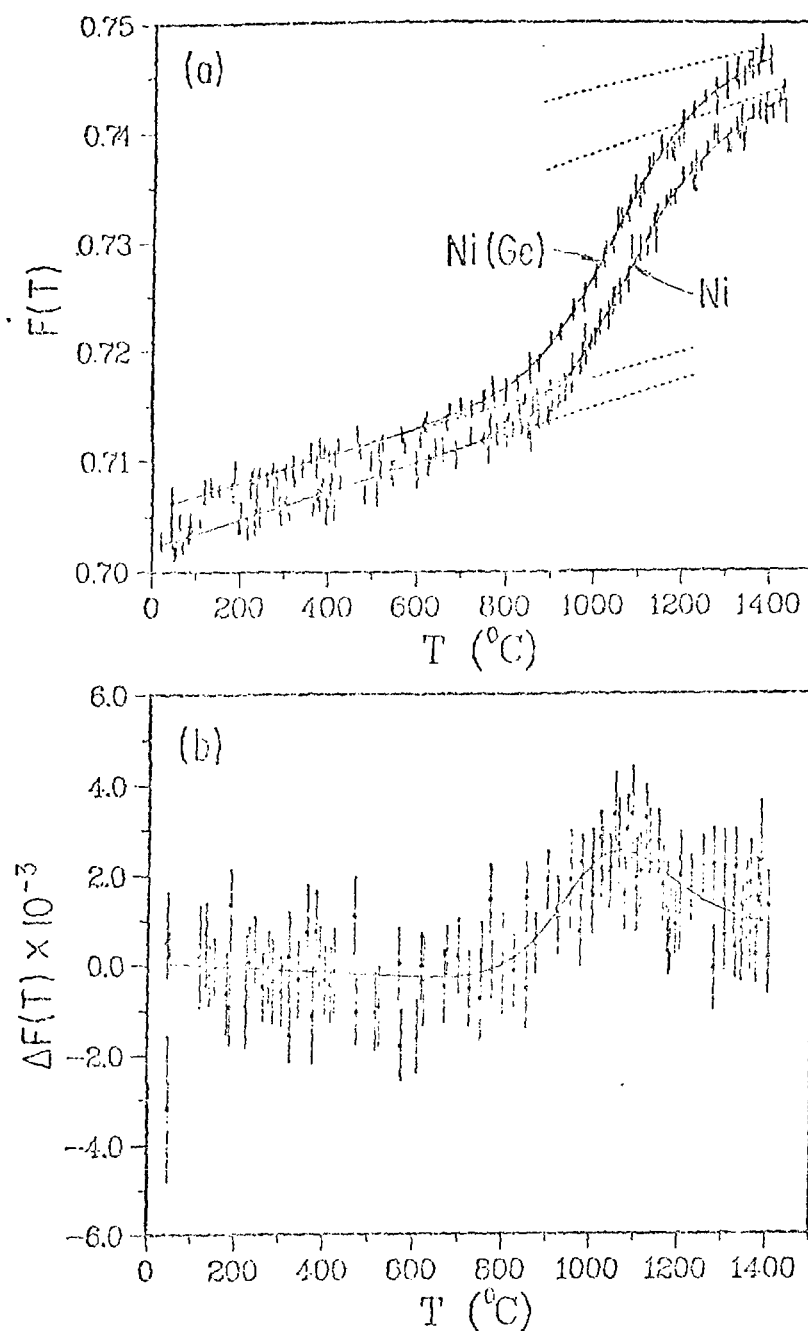


Fig. 7. (a) Doppler-broadening lineshape parameter  $F(T)$  for Ni and  $\text{Ni(1 at.\% Ge)}$  as a function of temperature, and the trapping model fits to these data. From Ref. 47.

(b) The difference  $\Delta F(T)$  between the data for the  $\text{Ni(1 at.\% Ge)}$  and the Ni shown in (a) as a function of temperature. From Ref. 48. This difference has been set to zero at the lowest temperature.

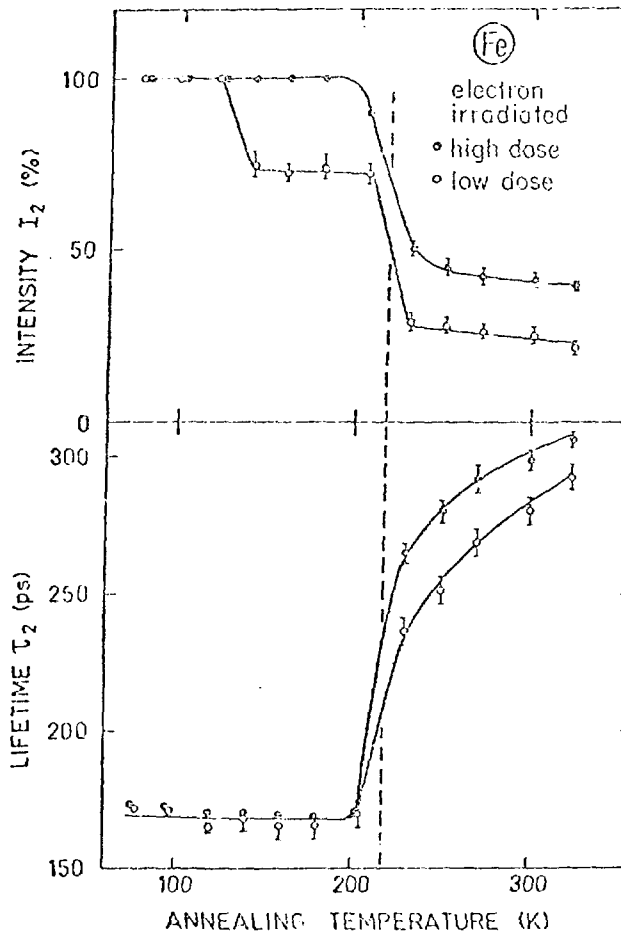


Fig. 8. The lifetime  $\tau_2$  of trapped positrons, and the intensity  $I_2$  of this component, in electron irradiated  $\alpha$ Fe as a function of annealing temperature. From Ref. 55.

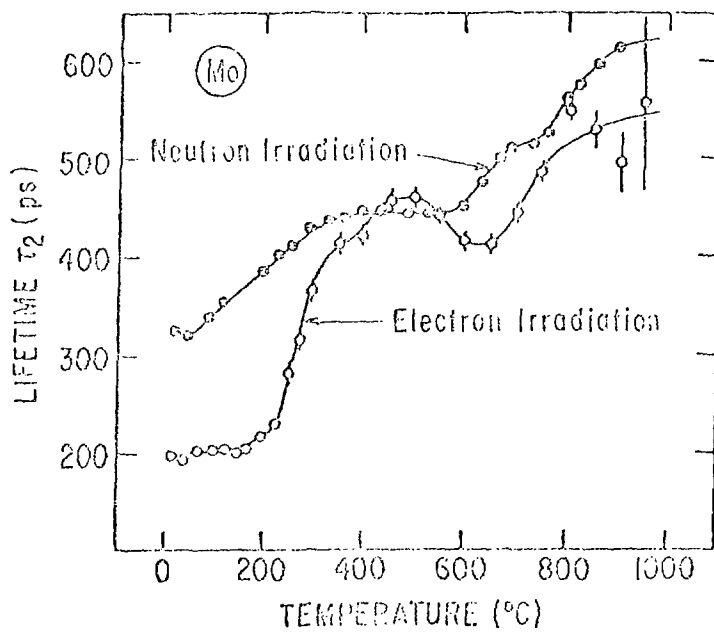


Fig. 9. Annealing behavior of the trapped-positron lifetime  $\tau_2$  in electron<sup>61</sup> and neutron<sup>62</sup> irradiated molybdenum. After Ref. 63.